#184 dup

FERMILAB-CONF-74-168-E #184

The Observation of Prompt Muons from Nucleon-Nucleon Interactions and A New Limit on the Production Cross Section for Massive Leptons*

D. Bintinger, J. Curry, J. Pilcher†

Enrico Fermi Institute

University of Chicago

D. Cheng, C. Rubbia, L. Sulak

Harvard University

W. Ford, A. K. Mann

University of Pennsylvania

A. Benvenuti, D. Cline, R. Imlay, P. Wanderer

University of Wisconsin

ABSTRACT

We have observed the direct production of muons in nucleon-nucleon collisions. The production cross section is 10^{-4} of the pion production cross section for both μ^+ and μ^-, and is insensitive to changes in transverse momentum and bombarding energy.

A limit for the production cross section of heavy penetrating leptons is given as a function of particle mass, momentum and lifetime.

Submitted to London Conference June 1974

We report preliminary results from an experiment in progress at the Fermi National Accelerator Laboratory to search for new short-lived massive leptons produced in nucleon-nucleon collisions. These leptons would be directly observed in the detector if their lifetime were sufficiently long. Alternatively, for short lifetimes, decay muons from the parents are sought. The experiment is also sensitive to muons produced directly in the hadron-hadron interaction. In this note we report the observation of "prompt" muons from the nucleon-nucleon collisions and present an upper limit on the production cross section for massive leptons entering the detector.

For maximum sensitivity to short-lifetime, low momentum leptons a compact detector was designed and situated 4.5 m downstream from the accelerator's internal target. The apparatus was sensitive to single penetrating leptons emitted at $\sim$ 90 mr in the laboratory with a transverse momentum in the range 0.85 to 2.0 GeV/c. Data were recorded over the continuous range of bombarding proton energy from 30 to 300 GeV. The normalization of the experiment was entirely internal by using the observed muons from pion and kaon decays.

Consider the technique used to detect muons from sources with a lifetime short compared to the pion lifetime. To observe these prompt muons at the level of a few parts in 10^4 of the pion flux, energetic pions and kaons were absorbed close to their production point before they had an appreciable decay probability. A shield of 21 absorption lengths was positioned as close to the target as possible. To measure

FERMILAB-CONF-74-168-E

and subtract the small remaining signal from hadron decay the first sections of the absorber were remotely controlled so the muon flux could be studied as a function of the available distance for hadron decay. An extrapolation to zero decay path has yeilded the flux of prompt muons.

A sketch of the experimental apparatus is shown in Fig. 1. The target consisted of thin filaments of carbon or polypropylene mounted on a disk rotating in the vertical plane below the beam. The fibers intercepted a fraction of the circulating proton beam in the main ring of the NAL accelerator. Particles produced in the target at laboratory angles close to 90 mr passed through a series of absorbers and into a magnetic spectrometer equipped with scintillation counters and multiwire proportional chambers. Two gas Čerenkov counters and two lead-glass Čerenkov counters were used for particle identification.

The first absorber element was a tungsten block which could be inserted or removed remotely. To minimize interactions in the tungsten of high energy forward going secondaries from the target, the block subtended a minimum production angle of 45 mr. With the block in place, the decay path for hadrons, including the absorption length of tungsten, was 40 cm. The remaining absorber was iron with a thickness variable in 10 cm steps. The longest hadron decay path employed was 110 cm, and with this setting the reduction in thickness of the iron absorber was 11%.

Particles emerging from the absorber at 84 mr to the beam direction entered a magnetic spectrometer. Three scintillation counters and 4 planes of multiwire proportional chambers were situated both upstream and

downstream of the magnet to define the track trajectories. The geometrical solid angle subtended by the detector was 21 μster.

The detector was located inside the accelerator's main ring tunnel just 4.5 m from the internal target. Because of the potentially harsh background conditions, extreme care was taken in the design and operation of detector elements. The timing and pulse height of each of the six triggering scintillators were recorded with each event and monitored with the on-line computer. The use of deadtimeless electronic logic allowed a continuous check of the accidental coincidence level in each counter. During normal data taking, the instataneous counting rates in the scintillators were never more than a few MHz. A typical timing curve for a single scintillator, with respect to the main coincidence, is shown in Fig. 2.

To measure the track trajectories, 8 planes of multiwire proportional chambers with 1 mm wire spacing were used. The redundancy of planes allowed a continuous check on the efficiency of each plane. Values of 95% were normal. The probability that a plane had extra wires struck was typically 8%.

To average over operating characteristics of the accelerator the absorber and/or magnet polarity were changed each hour. Regular runs were taken with the target removed and various absorber conditions.

The data presented here used a single setting of the spectrometer magnetic field. Both positive and negative particles were recorded simultaneously for all secondary momenta above 10 GeV. The field polarity of the spectrometer was reversed regularly to ensure equal detection

efficiency for particles of both charges.

Hadron contamination of the particles triggering the detector was found to be negligible from a consideration of the pulse height spectra of the two lead-glass Čerenkov counters. The two counters together with their housings represent 2.3 absorption lengths of material. A single, non-interacting charged particle with $\beta > 0.6$ produces a characteristic line spectrum in each counter. Tests in a hadron beam show that particles interacting in the counters produce a broad pulse height spectrum because of Čerenkov radiation of the charged secondaries. Fig. 3 shows the spectrum observed in one of the counters for a fraction of the present data. The observed line shape is entirely explained by the measured accidental spectrum and the calculated contribution from energetic δ-rays produced in the counter. There is no evidence for a significant excess at high pulse heights. This curve together with a study of the pulse height correlation between the two counters leads to an upper limit of 2% on the hadron contamination for all absorber conditions.

PART A. THE OBSERVATION OF PROMPT MUONS

Data were taken with five different hadron decay paths. The yield of hadron-decay muons in a given momentum interval is expected to increase linearly with decay path. The slope of the line is proportional to the initial hadron yield and inversely proportional to the momentum of the parents. We have measured this slope as a function of bombarding energy.

The results are shown in Fig. 4 together with predictions based on the pion production measurements of Carey et al.[1] and the K to π ratio measurement of Cronin et al.[2] The observations are in good agreement with expectation. The yield of μ^+ is significantly larger than μ^- because of the copious K^+ production at these transverse momenta.

To further confirm our understanding of the hadron production spectra and detector characteristics we have compared the observed muon momentum spectrum with that predicted from the measurements of references 1 and 2. In Fig. 5 the comparison is made for data taken with the longest decay path where the data is dominated by hadron decay. The detector's response is folded in by a Monte Carlo calculation. Again, the comparison is excellent.

Fig. 6 shows the relative muon yield as a function of decay path for negative muons in the momentum interval 20 to 25 GeV/c and averaged over bombarding energies from 60 to 300 GeV. The extrapolation to zero decay path shows a positive intercept of over 3 standard deviations.

The ratio of intercept to slope is directly proportioned to the ratio prompt muon yield to the pion yield. The proportionality constant is simply related to the hadron decay probability and measured π to K production ratios. Applying the necessary numerical factors, one obtains the results for prompt muon to pion cross sections given in Table I. These results assume the angular distribution of prompt muons and pions is the same over the effective apperture of the detector (± 6 mr). It should also be noted that results given in Table I represent only a fraction of the data of the final experiment. Results are presented for those kinematic

FERMILAB-CONF-74-168-E

regions most free of potential systematic effects.

We have considered the following systematic biases which might produce a non-zero intercept.

While the measurement does not rely on a knowledge of the absolute detection efficiency of the apparatus, it does require a knowledge of the relative efficiency for each absorber condition. Since the multiple scattering and ionization losses differ slightly between absorber conditions, this effect has been studied with a Monte Carlo calculation. For momenta above 20 GeV/c the efficiency does not vary significantly with absorber condition. For muon momenta in the interval 15 to 20 GeV/c a multiplicative correction factor of 1.12 must be applied to the yield measured with the shortest decay path to correct to an efficiency equal to that at the longest decay path.

We have studied the sensitivity of this relative correction to such factors as the initial hadron production spectrum, counter positions and other uncertainties in the detector geometry. For reasonable changes in these parameters there is no significant change in the relative efficiency. To ensure against coding errors in the Monte Carlo calculations, two independent programs were written at separate laboratories and run on separate computers. The results are in excellent agreement.

The quality of the acceptance calculation can be seen in Fig. 5, where the observed muon momentum spectrum is compared with the predicted spectrum. In another test of the acceptance calculation the tungsten absorber block was replaced by one of stainless steel. For the steel the radiation length is a factor of 5 smaller, so the multiple scattering

was significantly smaller. The point obtained corresponds to the second shortest decay path shown in Fig. 6 and agrees well with the linear fit. Other checks of the acceptance calculation include a comparison of the number of tracks bent up in the spectrometer to the number bent down, as well as a comparison with the observed event population across the multiwire proportional chambers.

A second source of bias we have considered is the production of muons from hadronic cascades within the absorber. This background is negligible because of the steeply falling transverse momentum spectrum of hadrons produced in the target and the energy degradation in the cascade process. For a detected muon of a given momentum, it is far more likely to have come from the decay of a pion produced in the target than from the hadronic cascade in the shield of a higher energy pion.

We have considered changes in the detector's performance as a function of decay path. The thickness of the shield changes from 21.4 absorption lengths, with the shortest decay path to 17 absorption lengths with the longest. Because the shield is thick and the relative change is modest, no changes in the detector performance as a function of decay path have been observed. In particular the multiwire proportional chamber efficiency and the probability of extra wires being struck are insensitive to the decay path.

The detector geometry has been carefully measured on several occasions. The beam position relative to the detector was monitored during the experiment to 0.5 mm. Absorption lengths which must be

added to the geometrical decay paths have been directly measured in the momentum range of this experiment at Serpukhov.[3]

In summary we can find no systematic biases to account for the positive intercepts.

Numerical results are given in Table I for prompt μ^+ and μ^- cross sections relative to pions. There is no significant dependence of the ratio on either muon transverse momentum, or muon charge.

The measurements reported here, combined with pion production cross sections,[2] give a Lorentz invariant production cross section for prompt muons of 6×10^{-33} cm^2/GeV^2 at a transverse momentum of 1.4 GeV/c.

Direct muon production has also been seen in several experiments at lower energies,[4-6] and in two other experiments at the Fermi Laboratory.[7-8]

PART B. LIMITS ON THE PRODUCTION OF HEAVY PENETRATING PARTICLES

We have searched for heavy penetrating particles with mass greater than 1 GeV/c^2 produced at 85 mr in the lab. Heavy particles would be identified by the absence of a pulse in each of the two threshold gas Čerenkov counters (Fig. 1). Cross section limits were obtained using the measured number of muons produced by pion and kaon decays and the published values of pion and kaon production cross sections. For heavy particles with a finite lifetime, a correction factor $C = \exp(LM/pc\tau)$ for decay must be applied to the cross section limits (L is the length of the detector, M the mass of the particle, p its momentum, and τ its

lifetime. The apparatus was made very short (10 m) so that it would have a good sensitivity even for particles with a mean decay path λ of a few meters. For example, for λ = 4m, C = 12, whereas if the detector were 100 m long, we would have $C = 7 \times 10^{10}$.

The variation of the cross section of any heavy penetrating particle with transverse momentum p_T is of course unknown, but may vary substantially with p_T. Thus it is important to obtain limits for both low and high values of p_T.

From a preliminary scan of the data we obtain the cross section limits shown in Table II. Limits are given for three bins of p_T for $\tau \to \infty$. The correction factor C for short-lived particles as a function of mass and lifetime is also shown.

We would like to acknowledge the support of the Fermi National Accelerator Laboratory and in particular D. Yovanovitch and his staff at the Internal Target Section. The following people also helped at various phases of the experiment: T. Y. Ling, R. Piccioni, D. Reeder, J. Sidles, A. Zylberstejn.

REFERENCES

1. D. C. Carey et al., Fermi Laboratory preprint NAL-74/48.
2. J. W. Cronin et al., Phys. Rev. Letters 31, 1426 (1973).
3. S. P. Denisov et al., Nuclear Physics B61, 62 (1973).
4. P. J. Wanderer et al., Phys. Rev. Letters 23, 729 (1969).
5. J. Christenson et al., Phys. Rev. Letters 25, 1523 (1970).
6. Bondarenko et al., Proceedings of XVI International Conference on High Energy Physics, Vol. 2, p. 329 (1972).
7. J. Boymond et al., Enrico Fermi Institute Preprint 74-24.
8. Fermi National Accelerator Laboratory experiment 70, unpublished.

*Work supported by the National Science Foundation and the U. S. Atomic Energy Commission

†An Alfred P. Sloan Foundation Fellow

FIGURE CAPTIONS

1. Experimental arrangement.
2. A typical timing curve showing the time separation of counts in one of the triggering scintillators with respect to the main 6-fold coincidence. The narrow peak corresponds to a count originating in-time with respect to the rest of the system.
3. Pulse height spectrum from the lead-glass Cerenkov counter used to monitor hadron contamination.
4. Relative μ^+ and μ^- yields arising from π and K decay as a function of bombarding energy. The smooth curves are predictions based on the hadron production measurements of references 1 and 2.
5. Observed muon momentum distribution for one setting of the spectrometer's magnetic field. The low momentum cut-off arises from the spectrometer acceptance. The dots correspond to the distribution expected from the hadron production measurements of references 1 and 2, folded with hadron decay, multiple scattering, and detector acceptance.
6. The observed muon yield as a function of decay path for μ^- mesons in the momentum intervals 20-25 GeV/c ($\langle P_\perp \rangle$ = 1.9 GeV/c). The data are averaged over bombarding energy from 60 to 300 GeV.

TABLE I

Muon Charge	Proton Energy Range (GeV)	Muon Momentum Range (GeV/c)	Average Muon Transverse Momentum (GeV/c)	Prompt Yield (x 10^{-4}) N_μ/N_π
(+)	60-300	15-20	1.4	.66±.28
(-)	60-300	15-20	1.4	.77±.30
(+)	60-300	> 20	1.9	.82±.35
(-)	60-300	> 20	1.9	1.24±.39
(+) +(-)	60-180	15-20	1.4	.094±.24
(+) +(-)	60-180	> 20	1.9	1.41±.54
(+) +(-)	180-300	15-20	1.4	1.05±.35
(+) +(-)	180-300	> 20	1.9	.48±.31

TABLE II

p_T	Correction factor For short-lived particles	Cross section limit for $\tau = \infty$ cm^2/GeV^2	Mass
.85 to 1.25 GeV	exp $[0.3 \times 10^{-8}\ M/\tau]$	2.6×10^{-34}	$M > .8\ GeV/c^2$
1.25 to 1.7	exp $[0.2 \times 10^{-8}\ M/\tau]$	1.7×10^{-35}	$M > 1.2\ GeV/c^2$
1.7 to 2.1	exp $[0.15 \times 10^{-8}\ M/\tau]$	7.3×10^{-36}	$M > 1.6\ GeV/c^2$

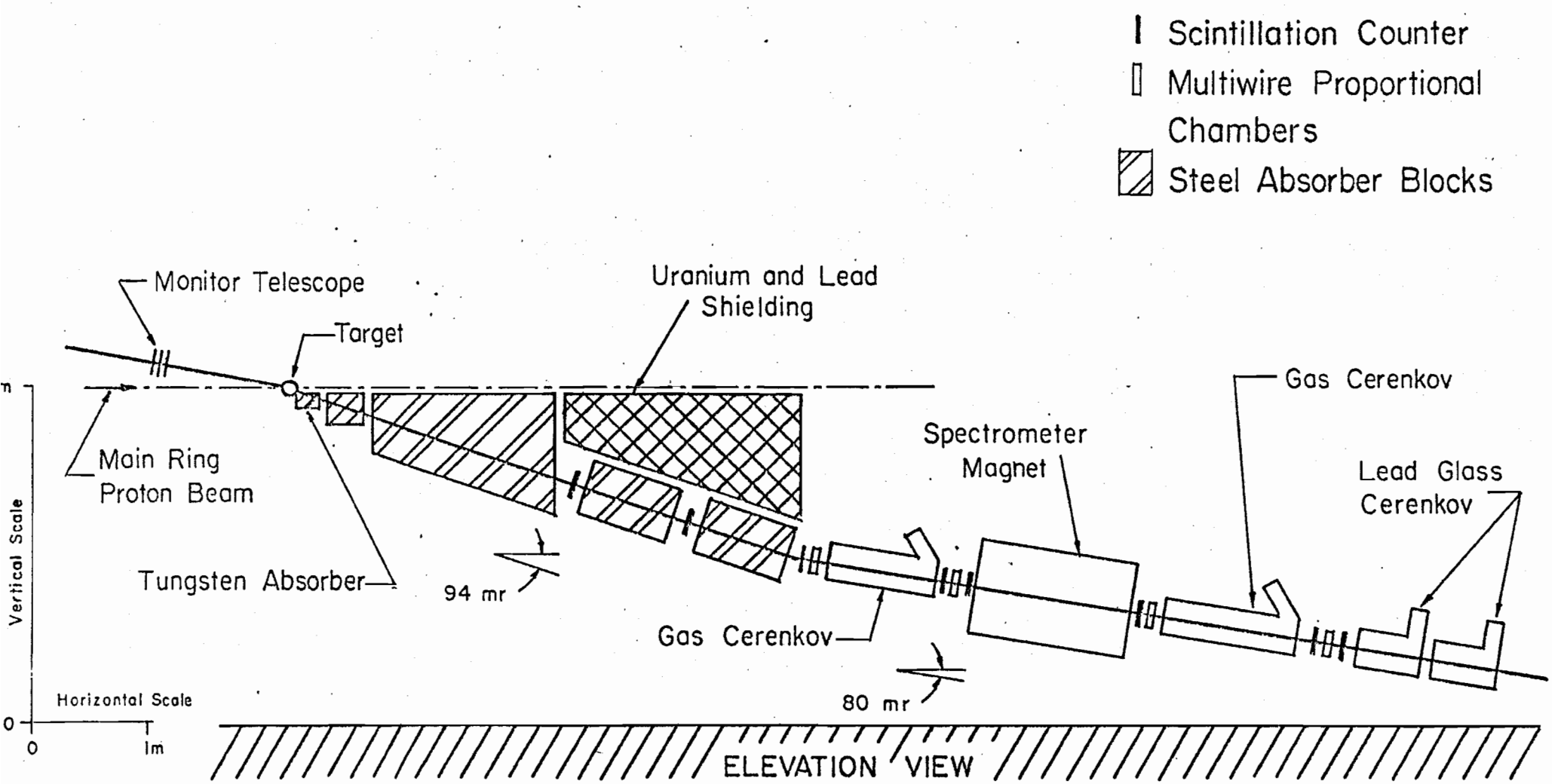
Scintillation Counter
Multiwire Proportional Chambers
Steel Absorber Blocks
Monitor Telescope
Target
Uranium and Lead Shielding
Main Ring Proton Beam
Tungsten Absorber
94 mr
Gas Cerenkov
Spectrometer Magnet
80 mr
Gas Cerenkov
Lead Glass Cerenkov
Vertical Scale
Horizontal Scale
0
0
1m
ELEVATION VIEW

FIGURE 1

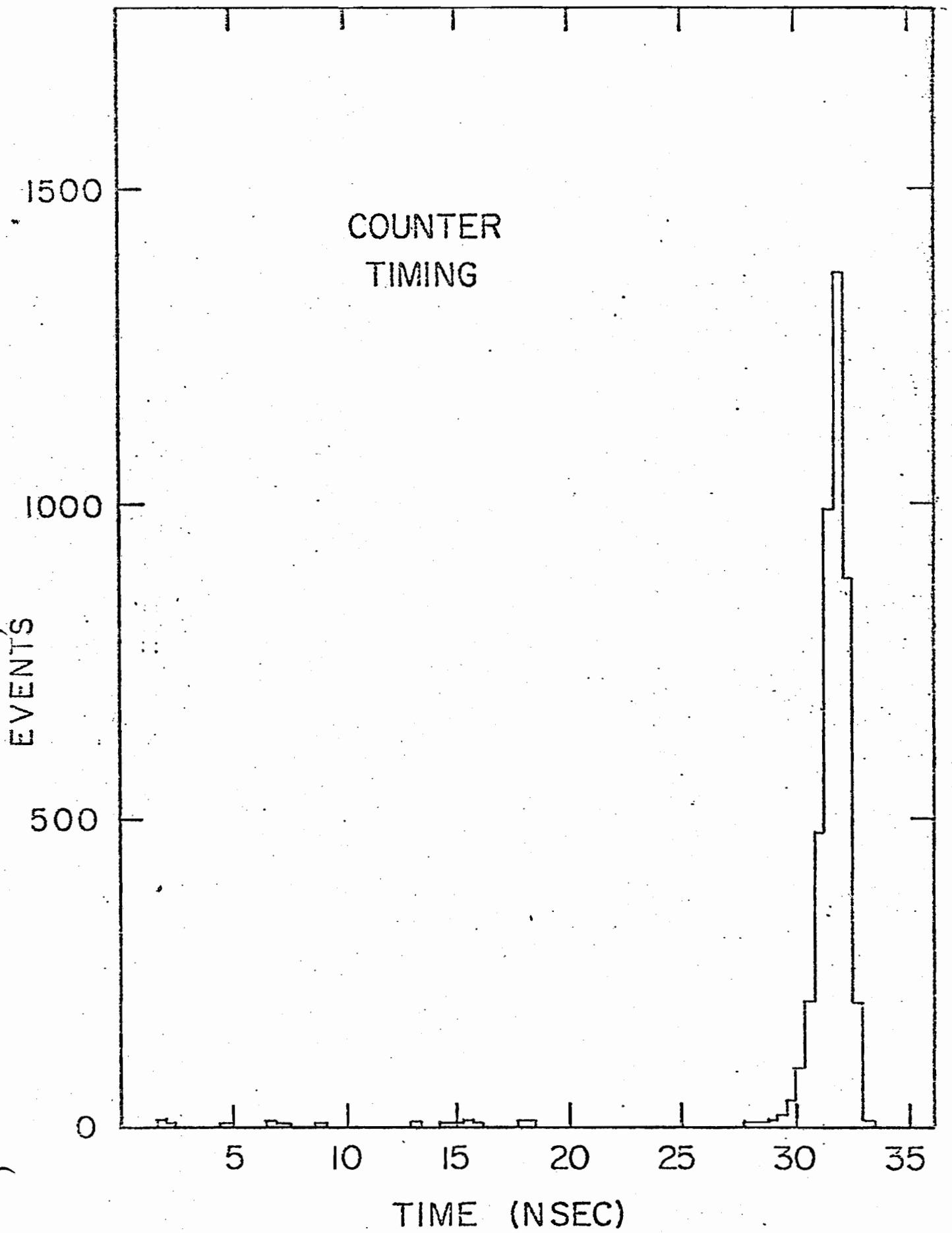
COUNTER
TIMING
1500
1000
500
0
EVENTS
5
10
15
20
25
30
35
TIME (NSEC)

FIGURE 2

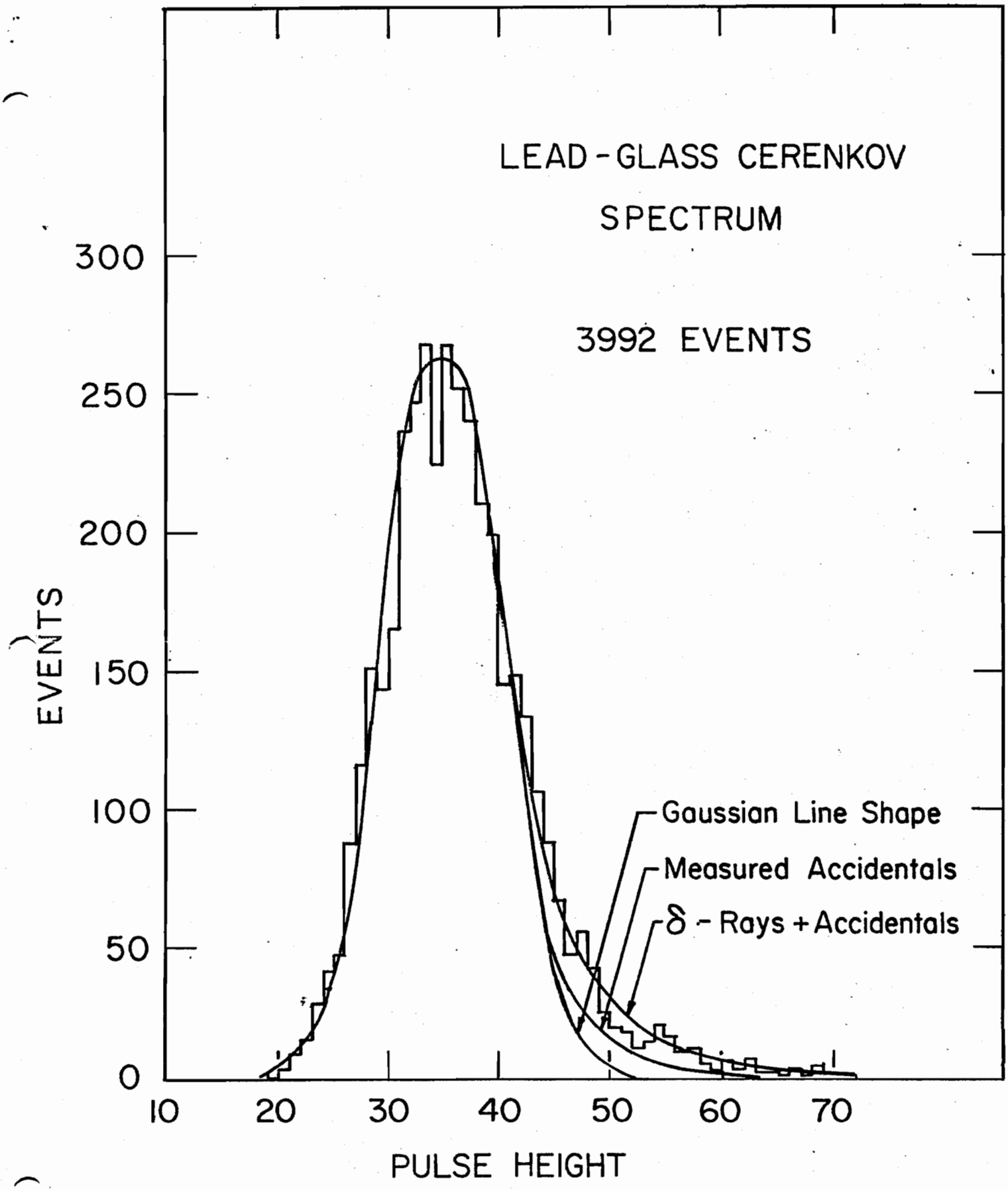
LEAD-GLASS CERENKOV
SPECTRUM
3992 EVENTS
Gaussian Line Shape
Measured Accidentals
δ - Rays + Accidentals
EVENTS
300
250
200
150
100
50
0
10
20
30
40
50
60
70
PULSE HEIGHT

FIGURE 3

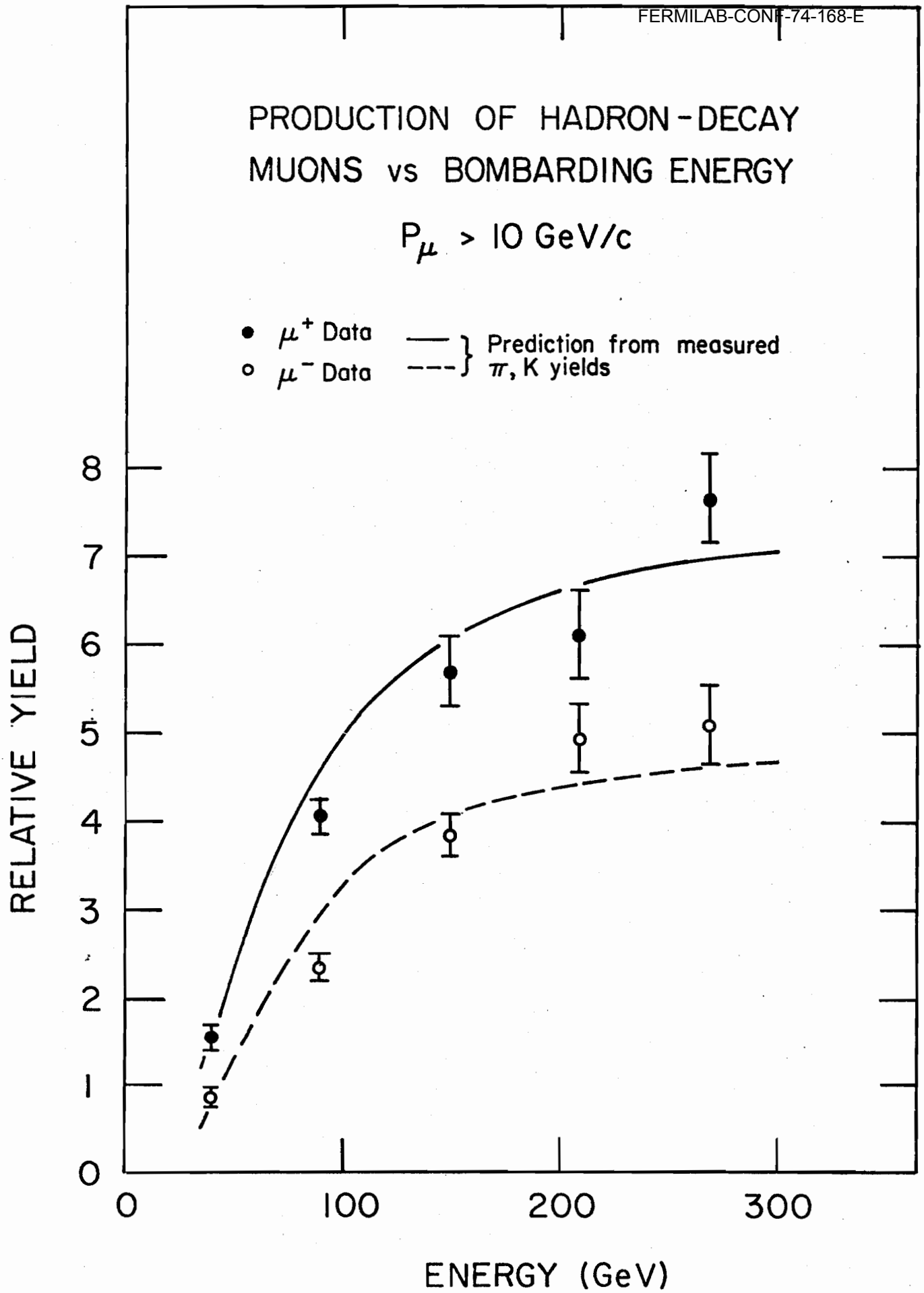
PRODUCTION OF HADRON-DECAY
MUONS vs BOMBARDING ENERGY
P_μ > 10 GeV/c
μ^+ Data
μ^- Data
Prediction from measured
π, K yields
RELATIVE YIELD
0
1
2
3
4
5
6
7
8
0
100
200
300
ENERGY (GeV)

FIGURE 4

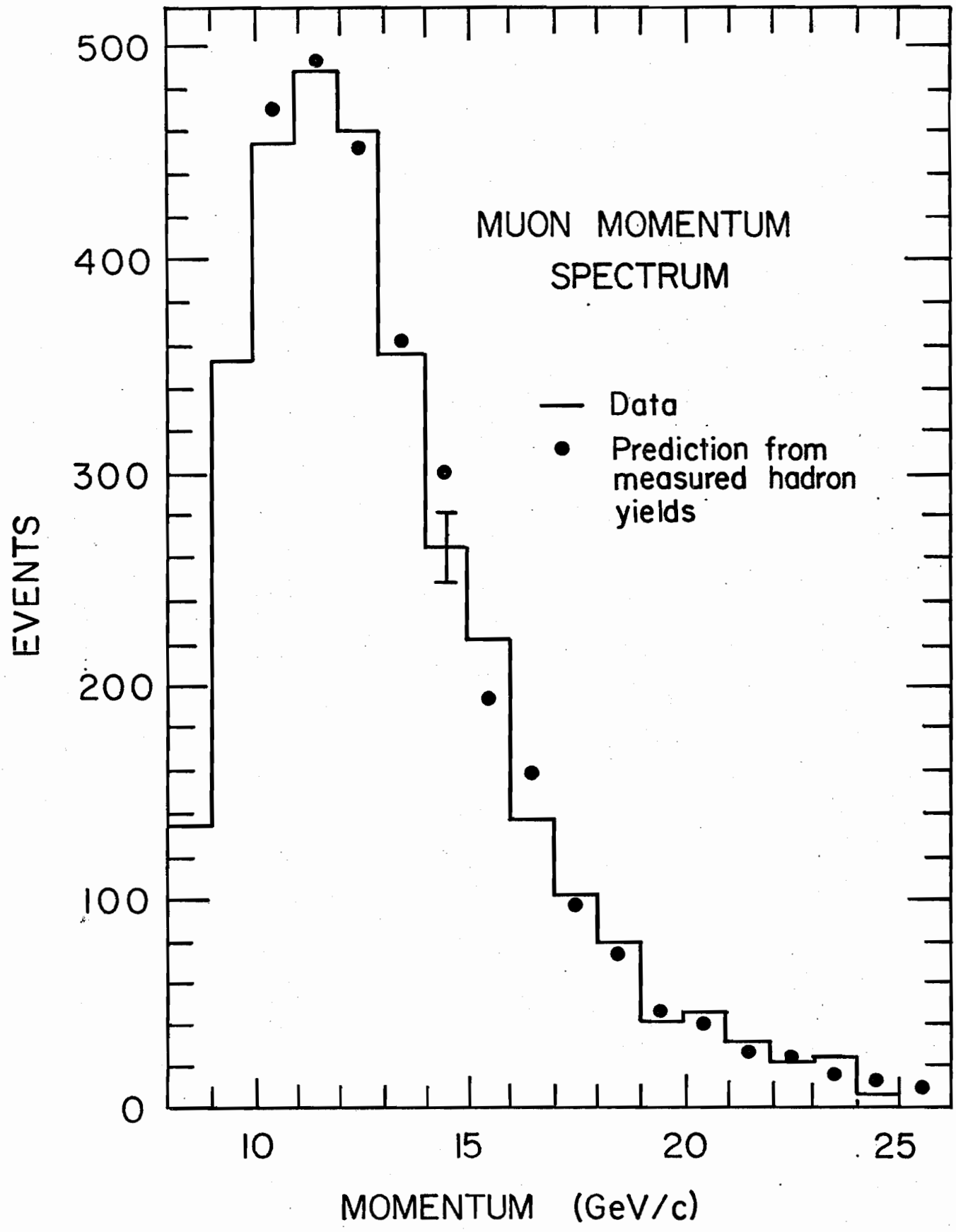
MUON MOMENTUM
SPECTRUM
Data
Prediction from measured hadron yields
EVENTS
500
400
300
200
100
0
10
15
20
25
MOMENTUM (GeV/c)

FIGURE 5

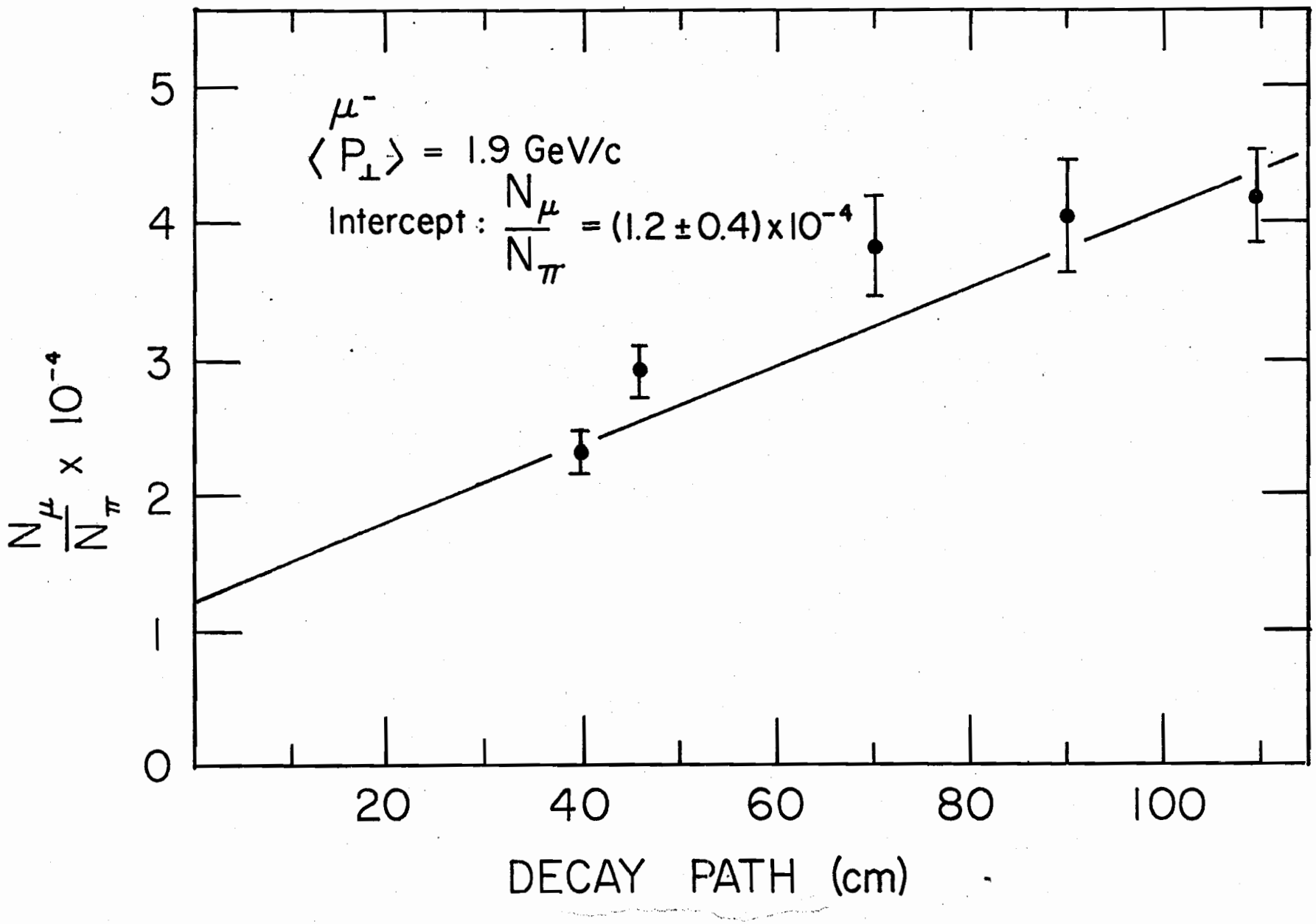
μ^-
$\langle P_\perp \rangle$ = 1.9 GeV/c
Intercept : $\frac{N_\mu}{N_\pi} = (1.2 \pm 0.4) \times 10^{-4}$
$N_\mu / N_\pi \times 10^{-4}$
0
1
2
3
4
5
20
40
60
80
100
DECAY PATH (cm)

FIGURE 6